

A COMPARATIVE STUDY OF SELECTED MODELS FOR EFFECTIVE THERMAL CONDUCTIVITY

Suren G. Aghbalyan¹, Vazgen Bagdasaryan², Gayane A. Vasilyan³,
Rafał Wyczółkowski⁴✉

¹Institute of Mining, Metallurgy and Chemical Technologies, National Polytechnic University of Armenia, Yerevan, Armenia

²Institute of Civil Engineering, Warsaw University of Life Sciences – SGGW, Warsaw, Poland

³Institute of Mining, Metallurgy and Chemical Technologies, National Polytechnic University of Armenia, Yerevan, Armenia

⁴Faculty of Production Engineering and Materials Technology, Czestochowa University of Technology, Czestochowa, Poland

ABSTRACT

This paper conducts a comparative evaluation of 22 models focusing on the effective thermal conductivity of two-phase porous materials. Calculations were performed for each model across a range of solid-to-fluid thermal conductivity ratios, spanning from 1 to 15,000, and for two different porosities: 0.1 and 0.2. The study advocates the use of dimensionless charts that normalised solid thermal conductivity (k_s) and effective thermal conductivity (k_{ef}) concerning fluid thermal conductivity (k_f) for qualitative analysis. Employing this approach, the examined models were categorised into four fundamental groups. The latter portion of the paper compares selected models with experimental data. These experiments involved testing eight porous media samples in the form of packed steel bars, arranged in two configurations: staggered and in-line. The tests were conducted over a temperature range of 75–400°C, corresponding to k_s -to- k_f ratios ranging from 1,800 to 855. Various graphical representations were used to compare measurement data with model calculations. The findings indicate that the most accurate comparisons can be made using linear charts, which present absolute values of the k_{ef} coefficient in relation to the thermal conductivity of the solid phase.

Keywords: thermal conductivity analysis, porous materials, cellular materials, heat exchange

INTRODUCTION

Porous and cellular materials are composite structures that consist of a solid framework that houses voids filled primarily with gas or fluid. Within this category, materials featuring metals as the solid phase represent a significant subgroup. The concept of porous and cellular metals was first introduced in the early 1970s, and they have found successful applications across various industries – including aviation (Öchsner, Murch & Lemos, 2008) and space exploration (Vujayakumur, 2004).

A fundamental physical property of these materials is their effective thermal conductivity, denoted as k_{ef} . This parameter encapsulates the intricate interplay of heat transfer mechanisms, including conduction through the solid phase, conduction through the gas phase and radiation within the void spaces (Wei, Zhang & Yu, 2009). Determining the effective thermal conductivity of cellular and porous materials is essential for tasks such as thermal design and numerical simulations. Consequently, research focusing on k_{ef} is crucial for numerous practical applications.

Several mathematical models have been developed to calculate k_{ef} . An important challenge in this field is comparing results obtained through different models. A widely accepted approach for this purpose is to normalise both the solid thermal conductivity (k_s) and effective thermal conductivity (k_{ef}) with respect to the thermal conductivity of the fluid (k_f), yielding dimensionless charts (Van Antwerpen, du Toit & Rousseau, 2010). However, it is worth noting that drawing conclusions based solely on such diagrams can be misleading due to the use of logarithmic scales. This paper seeks to delve into these issues in greater depth. As a result, we present model-based computations in various formats. An essential aspect of our analysis involves comparing of model-derived k_{ef} values with our own results from experimental measurements.

MATERIAL AND METHODS

In this study, we examined 22 distinct effective thermal conductivity models. The presentation of these models is limited to their names. However, the complete mathematical equations and details regarding the methodology and assumptions used in their derivation can be found in the provided references. In Table 1, we list the models that were analysed in this study to assess effective thermal conductivity.

The Parallel and Series models represent the upper and lower limits of k_{ef} and serve as reference bounds for the other correlations. The models under consideration can be categorised into two main groups. The first group comprises rigid models, which are solely functions of thermal conductivities and porosity. The second group consists of flexible models, which include additional parameters. Notably, the flexible category encompasses two Miller models, the Kunii–Smith model and the Krischer model (Carson, Lovatt, Tanner & Cleland, 2006).

In calculating the k_{ef} coefficient, a thermal conductivity value of $0.0257 \text{ W}\cdot\text{m}^{-1}\cdot\text{K}^{-1}$ was adopted for k_f , representing the thermal conductivity of air. The value of k_s was varied across a range from 0.0257 to $386 \text{ W}\cdot\text{m}^{-1}\cdot\text{K}^{-1}$, with the upper limit corresponding to copper. Under these assumptions, the ratio of conductivity (k_s/k_f) was examined across a spectrum

Table 1. Models examined for effective thermal conductivity

| Name of the model | References |
|--------------------------|---|
| Parallel | |
| Series | |
| Maxwell Upper Bound | Wang, Carson, North and Cleland (2006) |
| Maxwell Lower Bound | |
| Effective Medium Theorem | |
| Horai | Horai (1991) |
| Beck | Beck and Beck (1965) |
| Chang | Chang (1982) |
| Assad | Assad (1995) |
| Woodside | Woodside and Messmer (1961) |
| Bruggeman | Abereshi, Goharshadi, Zebarjad, Fadafan and Youssefi (2010) |
| Miller Upper Bound | Miller (1969) |
| Miller Lower Bound | |
| Kunii–Smith | Kunii and Smith (1960) |
| Zehner–Schlunder | Zehner and Schlunder (1970) |
| Krupiczka | Krupiczka (1967) |
| Levy | Levy (1981) |
| Kopelman | Kopelman (1966) |
| Hill | Hill, Leitman and Sunderland (1967) |
| Rayleigh | Pietrak and Wiśniewski (2015) |
| Krischer | Krischer (1956) |

Source: own work.

from 100 to 1.5×10^4 . Calculations for each model were conducted for two distinct porosities, namely 0.1 and 0.2, representing granular media composed of cylindrical particles arranged in a staggered and in-line configuration, respectively.

As part of the analysis, a critical aspect involved comparing the model calculations with experimental results. To achieve this, we utilised measurements conducted on packed steel bar beds (as reported by Wyczółkowski in 2017). These beds represent two-phase granular media composed of steel and air. The examinations specifically concentrated on two distinct bar arrangements: staggered (with a porosity of 0.1) and in-line (with a porosity of 0.2).

The samples for each type of bed consisted of bars with varying diameters: 10, 20, 30 and 40 mm. Measurements were carried out for each sample over a temperature range spanning from 75° to 400°C .

RESULTS AND DISCUSSION

The calculated effective thermal conductivity values were initially presented in dimensionless logarithmic diagrams. For clarity, we have presented eight separate diagrams on each figure (Fig. 1 for porosity 0.1 and Fig. 2 for porosity 0.2). In each diagram, we have included results obtained for the boundary models, namely the Parallel and Series models, with the results of other models positioned in between. These diagrams effectively illustrate how the coefficient k_f changes for individual models based on variations in the k_s -to- k_f ratio. However, it is essential to note that data presented in this format primarily provides qualitative information. This makes it challenging to precisely determine the extent of differentiation between individual models.

To address this, we grouped the considered models into several categories. The first group, labelled ‘Upper’, consists of models closely resembling the Parallel model. This group was further subdivided into two subgroups: ‘Upper A’, encompassing models very similar to the Parallel model, including Maxwell UB, EMT, Bruggeman, Kopelman, Miller UB 1/9 and Krischer 0.0001, and ‘Upper B’, consisting of models that are less similar to the Parallel model, such as Horai, Levy, Hill, Miller UB 1/3 and Krischer 0.001.

The second group, termed ‘Lower’, comprises models with results closely resembling the Series model, particularly for which the conductivity ratio does not exceed 50 across the entire range of k_s . Models within this group include Maxwell LB, Woodside, Rayleigh and Miller LB 1/3.

The third group encompasses models with results in the dimensionless diagrams that exhibit profiles similar to the Series model. However, these models predict conductivity ratios close to or greater than 50 across the entire k_s range and are denoted as ‘Mean’. This group includes Zehner–Schlunder, Miller LB 1/9, all Kunii-Smith models and Krischer 0.1.

The last group, termed ‘Residual’, includes models with results falling between the ‘Upper’ and ‘Mean’ models, represented by Beck, Assad, Krupiczka and Krischer 0.01. These categorisations help provide a structured framework for understanding the differences among the models.

Figure 1 presents dimensionless logarithmic diagrams illustrating the values of k_{ef} obtained for a porosity of 0.1 and, in Figure 2, for a porosity of 0.2. Each diagram within this figure showcases the variation in k_{ef} values across the examined models, with the Parallel and Series models as reference boundaries. These diagrams offer a qualitative representation of how individual models respond to changes in the k_s -to- k_f ratio. However, it’s important to note that these charts primarily convey qualitative information. For a more precise understanding of the differences between the models, they were categorised into several groups (as discussed earlier).

New diagrams have been created to showcase the quantitative distinctions among individual models (see Figs 3 and 4). These diagrams portray variations in the k_{ef} coefficient concerning k_s , spanning from 25.7 to 257 W·m⁻¹·K⁻¹. The lower end of this range corresponds to high-alloy steel, while the upper limit represents pure aluminium. These diagrams are instrumental in providing a more precise understanding of the differences between the models.

For the models in the Upper A group, it was observed that an increase in porosity led to greater discrepancies between the results obtained by individual models. Within this group, the Kopelman model exhibited the closest similarity to the Parallel model, while the EMT and Bruggeman models were the least similar. Considerably greater variations were noticed within the Upper B group. The results of the Miller and Horai models remained unaffected by changes in porosity, whereas other models in this category demonstrated sensitivity to porosity variations. Among the Upper models, the Hill model was the closest to the upper bound, while the Levy model deviated the furthest from this boundary. What is common among all Upper models, except for Krischer, is that the k_{ef} values they predict increase as the thermal conductivity of the solid phase, k_s , increases. This suggests that solid-phase conduction is the primary mechanism of heat transfer in these models. Moreover, for all models in this category (except Krischer), the increase in the k_{ef} coefficient versus k_s is linear, and the discrepancies in results compared to the Parallel model do not intensify with

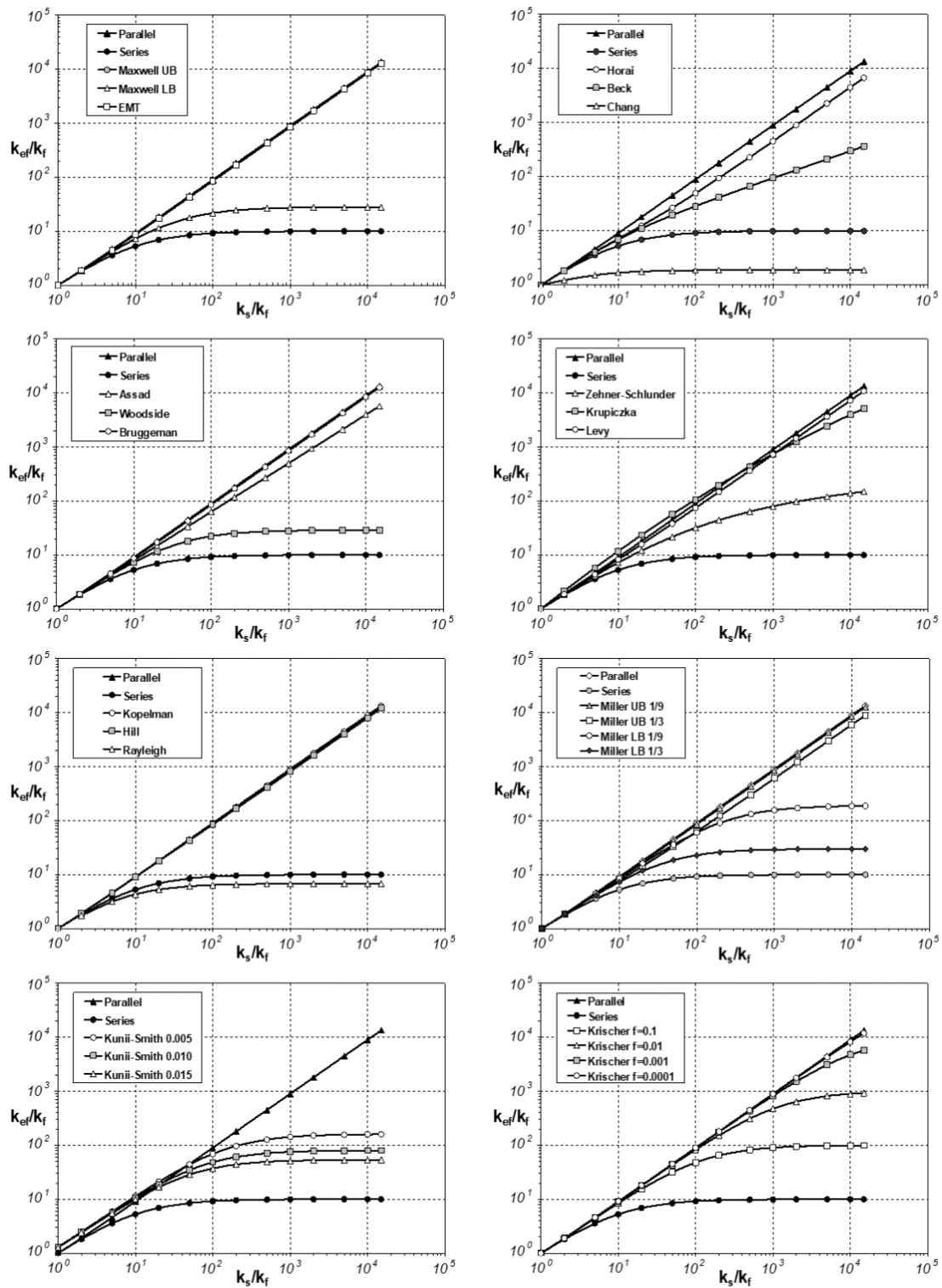


Fig. 1. Dimensionless logarithmic charts of effective thermal conductivity (k_{ef}) values for porosity 0.1

Source: own work.

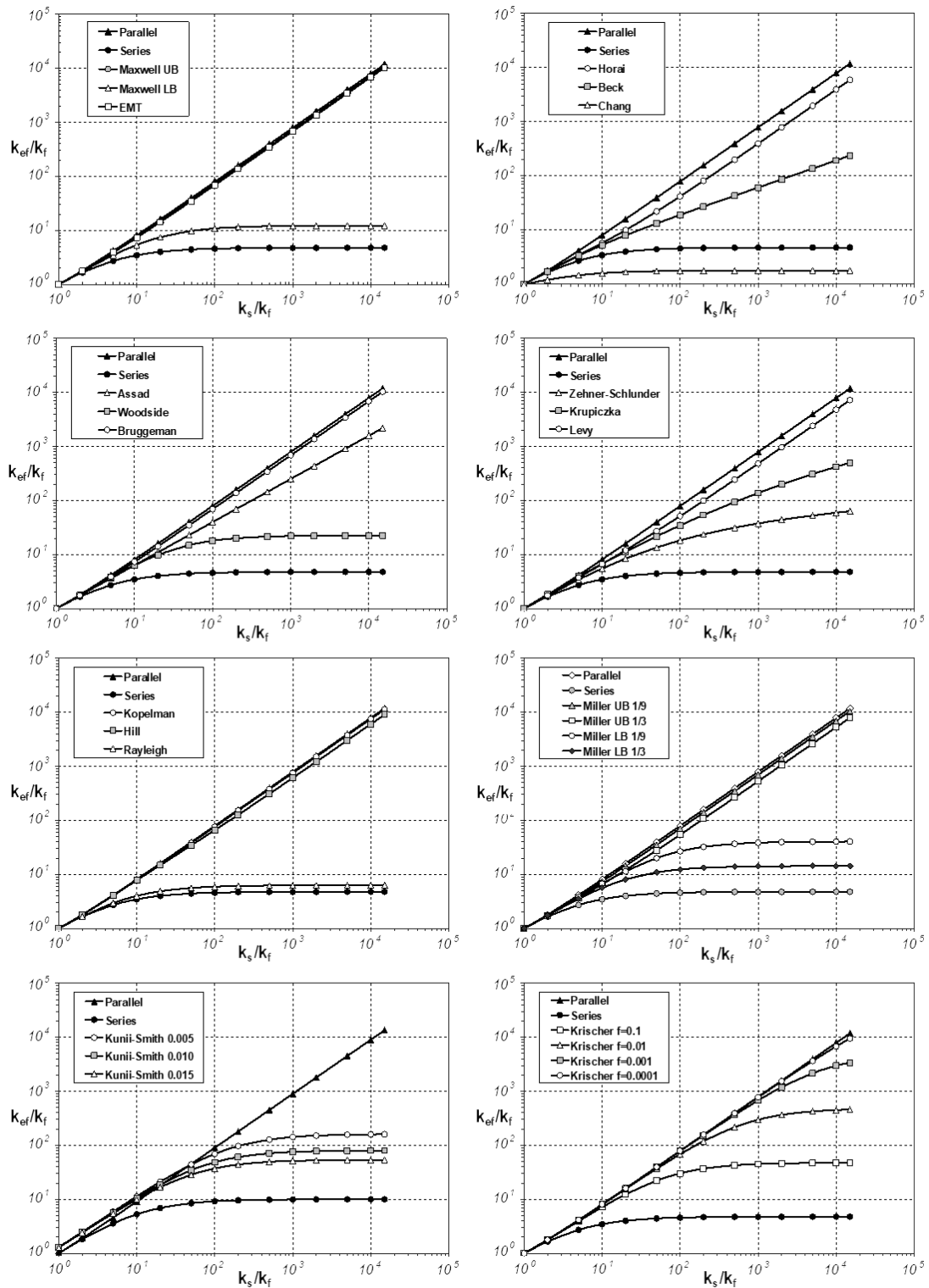


Fig. 2. Dimensionless logarithmic charts of effective thermal conductivity (k_{ef}) values for porosity 0.2
Source: own work.

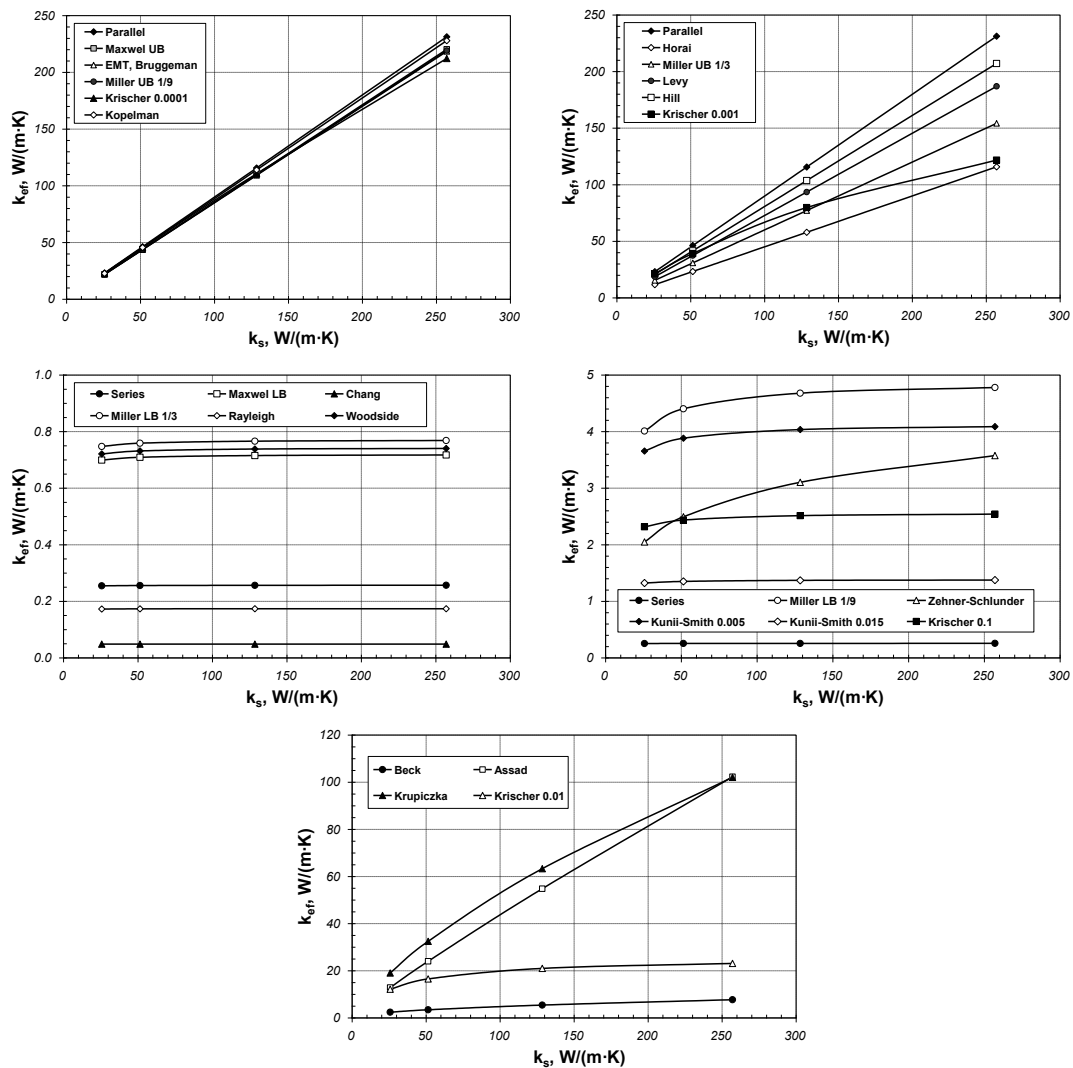


Fig. 3. Effective thermal conductivity (k_{ef}) versus normalised solid effective conductivity (k_s) calculation for porosity 0.1

Source: own work.

an increasing k_s . In the Krischer model, the increase in k_{ef} dynamics reduces with higher k_s values.

In the case of Lower models, the k_{ef} coefficient remained unchanged with varying k_s . This implies that these models primarily rely on fluid-phase conduction as the dominant heat transfer mechanism. Mean models, similarly to Lower models, respond to porosity changes but do not exhibit substantial variations as the thermal conductivity of the solid phase increases. However, one exception is the Zehner–

–Schlunder model, which responds to changes in k_s , particularly at low porosities.

Except for the Beck model, the results for the residual models exhibited a strong dependence on porosity, with the most significant effect observed among all the specified groups. Additionally, for all four models in this category, the k_{ef} coefficient increased as the thermal conductivity of the solid phase (k_s) rose. This indicates that solid-phase conduction is primary heat transfer mechanism in these models.

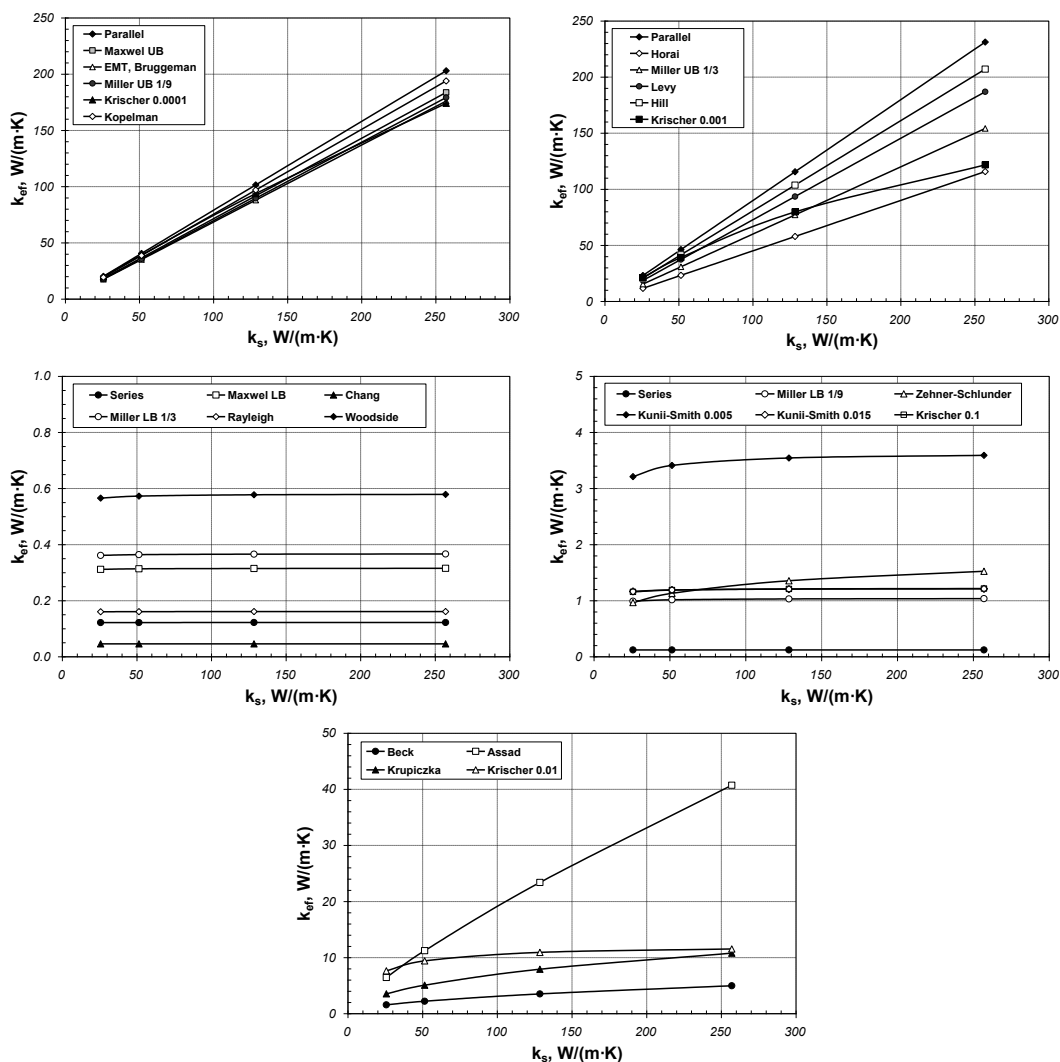


Fig. 4. Effective thermal conductivity (k_{ef}) versus normalised solid effective conductivity (k_s) calculation for porosity 0.2

Source: own work.

As previously mentioned, another essential analysis aspect involved comparing the model calculations with experimental results. The results of these measurements are presented in Figure 5, where Figure 5a pertains to staggered samples and Figure 5b pertains to in-line samples.

To facilitate the comparison of experimental data with model values of k_{ef} , additional calculations were necessary. These calculations required information about the coefficients k_s and k_f which pertain

to low-carbon steel and air for the bar beds. The variations in the k_s and k_f values with respect to temperature are described by the following relationships (Wyczółkowski, 2017):

$$k_s = 1.24 \cdot 10^{-8} t^3 - 3.26 \cdot 10^{-5} t^2 - 1.19 \cdot 10^{-2} t + 51.35, \quad (1)$$

$$k_f = -2.882 \cdot 10^{-8} t^2 + 8.051 \cdot 10^{-5} t + 0.02. \quad (2)$$

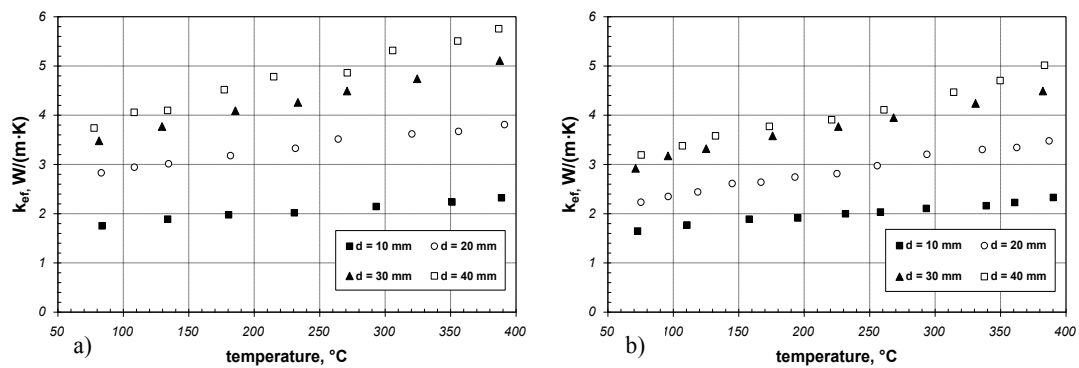


Fig. 5. Experimental results of effective thermal conductivity (k_{ef}): a – values for staggered samples; b – values for in-line samples

Source: own work.

Within the temperature range considered in the experimental investigations, the k_s -to- k_f ratio for the samples ranged from 856 to 1,681. For each sample, the changes in the k_{ef} -to- k_f ratio are presented as logarithmic diagrams, as shown in Figure 6a for staggered samples and Figure 7a for in-line samples.

It was observed that the results obtained for samples with a porosity of 0.1 closely resemble those of eight models: Maxwell LB, Beck, Woodside, Miller LB 1/3, all cases of Kunii–Smith, Zehner–Schlunder and Krischer 0.1. Moreover, the results obtained for samples with a porosity of 0.2 are akin to five models: Beck, all cases of Kunii–Smith, Zehner–Schlunder and Krischer 0.05. The

values obtained for these models are presented in Figure 6b for staggered samples and Figure 7b for in-line samples.

Figures 8 and 9 display variations in the k_{ef} coefficient in dimensional form concerning k_s . Among all the presentation methods, this form is the most convenient for analysis. When considering the staggered beds, the best match is observed between the 20-millimetre sample and the Zehner–Schlunder model. In the case of in-line beds, the most accurate alignment is found between the 20-millimetre sample and the Kunii–Smith 0.1 model.

Based on the results of the examinations, it is evident that linear diagrams with data presented in

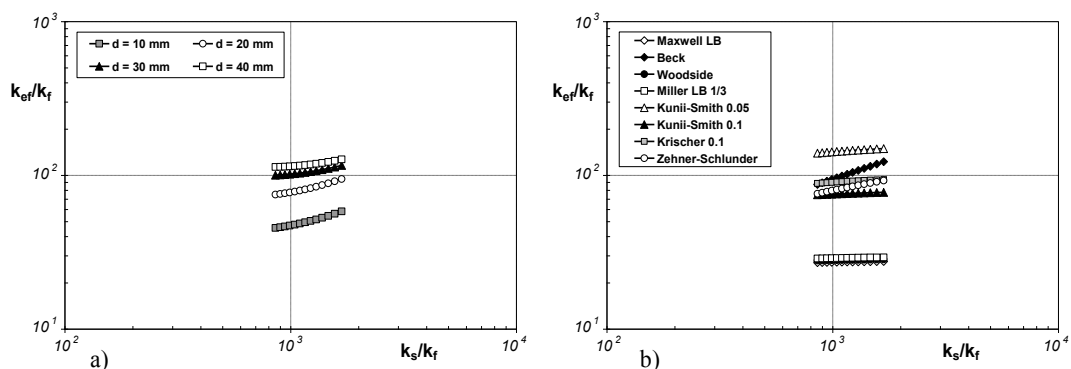


Fig. 6. Comparison of values of effective thermal conductivity (k_{ef}) in dimensionless logarithmic charts for porosity 0.1: a – experimental data; b – model results

Source: own work.

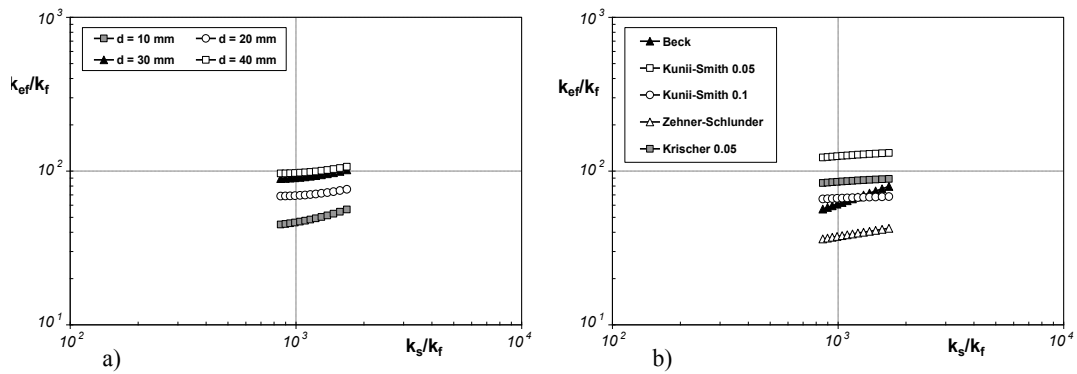


Fig. 7. Comparison of values of effective thermal conductivity (k_{ef}) in dimensionless logarithmic charts for porosity 0.2: a – experimental data; b – model results

Source: own work.

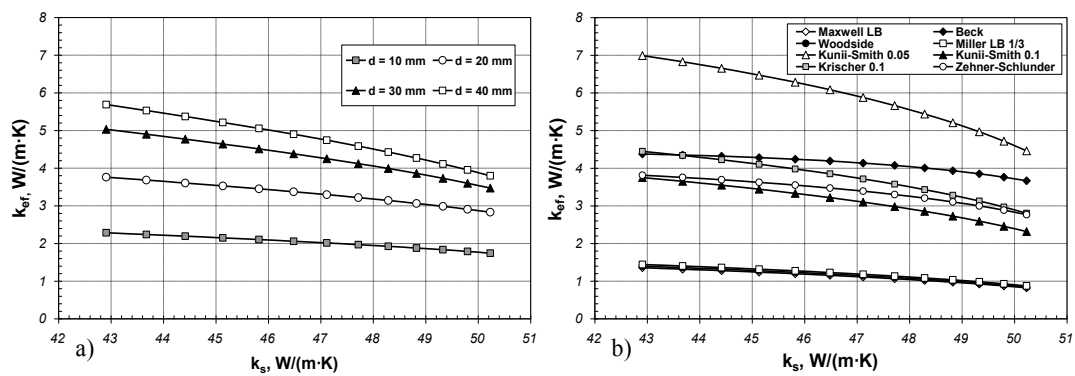


Fig. 8. Comparison of values of effective thermal conductivity (k_{ef}) in dimensional form (k_{ef} versus k_s) in the linear charts for porosity 0.1: a – experimental data; b – model results

Source: own work.

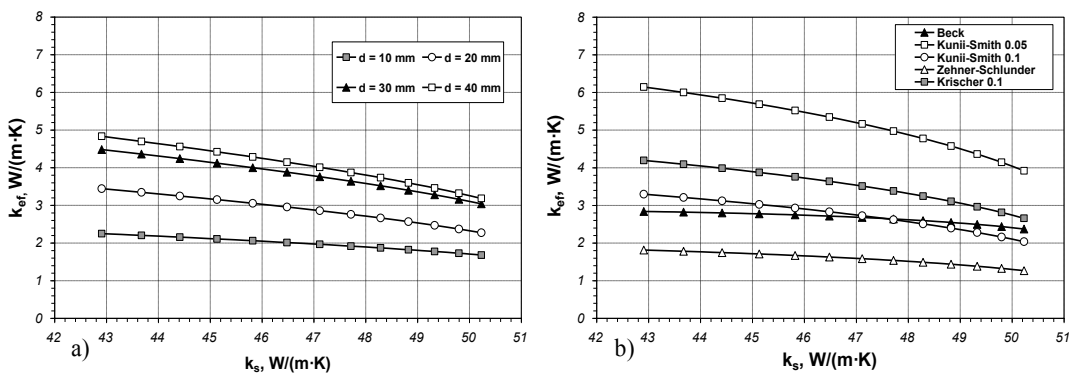


Fig. 9. Comparison of values of effective thermal conductivity (k_{ef}) in dimensional form (k_{ef} versus k_s) in the linear charts for porosity 0.2: a – experimental data; b – model results

Source: own work.

dimensional form are the most convenient for conducting comparative analyses of effective thermal conductivity. This approach is particularly effective when the analysed values of k_{ef} , k_s and k_f change over relatively smaller ranges. In instances where these values cover larger or more extensive ranges, using of logarithmic scales becomes necessary.

CONCLUSIONS

The comparison of various models of effective thermal conductivity is a significant concern within the field of thermophysics of porous media. This paper has provided a comprehensive analysis of 22 computational models for this parameter. It was evident that logarithmic dimensionless diagrams should primarily be used for qualitative comparisons. Comparing results obtained from models with experimental data can be particularly challenging and less transparent. Other types of diagrams should be employed to perform quantitative comparisons between specific models or with experimental data.

The suitability of using linear diagrams depends on the range of changes in the coefficients k_{ef} , k_s and k_f for the materials in question. Linear scales are preferable when these ranges are not excessively wide. However, when dealing with extended ranges, it is advisable to create several separate charts for narrower ranges of changes in these coefficients. For the most accurate comparisons, linear diagrams should be employed as they present changes in the absolute values of effective thermal conductivity as functions of thermal conductivity – k_s or k_f .

Authors' contributions

Conceptualisation: R.W., S.A. and V.B.; methodology: R.W. and G.V.; validation: S.A. and V.B.; formal analysis: R.W. and G.V.; investigation: R.W. and V.B.; writing – original draft preparation: R.W. and S.A.; writing – review and editing: V.B. and G.V.; visualisation: V.B. and G.V.; supervision: S.A. and R.W.

All authors have read and agreed to the published version of the manuscript.

REFERENCES

- Abareshi, M., Goharshadi, E. K., Zebarjad, S. M., Fadafan, H. K. & Youssefi, A. (2010). Fabrication, characterization and measurement of thermal conductivity of Fe_3O_4 nanofluids. *Journal of Magnetism and Magnetic Materials*, 322 (4), 3895–3901.
- Assad, A. (1955). *A Study of Thermal Conductivity of Fluid Bearing Porous Rocks* (doctoral thesis). University of California, Berkeley, California.
- Beck, J. N. & Beck, A. E. (1965). Computing thermal conductivities of rocks from chips and conventional specimen. *Journal of Geophysical Research*, 70 (20), 5227–5239.
- Carson, J. K., Lovatt, S. J., Tanner, D. J. & Cleland, A. C. (2006). Predicting the effective thermal conductivity of unfrozen, porous foods. *Journal of Food Engineering*, 75 (3), 297–307.
- Chang, H-C. (1982). Multi-scale analysis of effective transport in periodic heterogeneous media. *Chemical Engineering Communications*, 15 (4), 83–91.
- Hill, J. E., Leitman, J. D. & Sunderland J. E. (1967). Thermal conductivity of various meats. *Food Technology*, 21, 1143–1148.
- Horai, K. (1991). Thermal conductivity of Hawaiian basalt: A new interpretation of Robertson and Peck's data. *Journal of Geophysical Research*, 96 (B3), 4125–4132.
- Kopelman, I. J. (1966). *Transient heat transfer and thermal properties in food system* (PhD dissertation). Michigan State University, East Lansing.
- Krischer, O. (1956). *Die wissenschaftlichen Grundlagen der Tracknungstechnik* (1st ed.). Berlin: Springer-Verlag.
- Krupiczka, R. (1967). Analysis of thermal conductivity in granular materials. *International Chemical Engineering*, 7 (1), 122–144.
- Kunii, D. & Smith, J. M. (1960). Heat transfer characteristics of porous rocks. *AIChE Journal*, 6 (1), 71–78.
- Levy, F. L. (1981). A modified Maxwell-Eucken equation for calculating the thermal conductivity of two-component solutions or mixtures. *International Journal of Refrigeration*, 4 (4), 223–225.
- Miller, M. N. (1969). Bounds for effective electrical, thermal, and magnetic properties of heterogeneous materials. *Journal of Mathematical Physics*, 10, 1988–2004.
- Öchsner, A., Murch, G. & Lemos, M. de (2008). *Cellular and Porous Materials Thermal Properties Simulation and Prediction*. Weinheim: Wiley-VCH Verlag.

- Pietrak, K. & Wiśniewski, T. (2015). A review of models for effective thermal conductivity of composite materials. *Journal of Power Technologies*, 95 (1), 14–24.
- Van Antwerpen, W., Toit, C. G. du & Rousseau, P. G. (2010). A review of correlations to model the packing structure and effective thermal conductivity in packed beds of mono-sized spherical particles. *Nuclear Engineering and Design*, 240, 1803–1818.
- Vijayakumar, S. (2004). Parametric based design of CFRP honeycomb sandwich cylinder for a spacecraft. *Composite Structures*, 65 (1), 7–12.
- Wang, J., Carson, J. K., North, M. F. & Cleland, D. J. (2008). A new structural model of effective thermal conductivity for heterogeneous materials with co-continuous phases. *International Journal of Heat and Mass Transfer*, 51 (9–10), 2389–2397.
- Wei, G., Zhang, X. & Yu, F. (2009). Effective thermal conductivity analysis of xanotlite-aerogel composite insulation material. *Journal of Thermal Science*, 18 (2), 142–149.
- Woodside, W. & Messmer, J. (1961). Thermal conductivity of porous media. *Journal of Applied Physics*, 32, 1688–1768.
- Wyczółkowi, R. (2017). *Modelowanie efektywnej przewodności cieplnej z wykorzystaniem pojęcia oporu termicznego*. Częstochowa: Wydawnictwo WIPiTM Politechniki Częstochowskiej.
- Zehner, P. & Schlunder, E. U. (1970). Thermal conductivity of granular materials at moderate temperatures. *Chemie Ingeieur Technik*, 42, 933–941.

ANALIZA PORÓWNAWCZA WYBRANYCH MODELI PRZEWODNICTWA CIEPLNEGO

STRESZCZENIE

W niniejszej pracy przeprowadzono analizę porównawczą 22 modeli skoncentrowanych na efektywnym przewodnictwie cieplnym dwufazowych materiałów porowatych. Obliczenia zostały wykonane dla każdego modelu w zakresie stosunku przewodnictwa cieplnego ciała stałego do płynu (wahającego się od 1 do 15 000) oraz dla dwóch różnych porowatości (0,1 i 0,2). Badanie prezentuje wykorzystanie bezwymiarowych wykresów normalizujących przewodnictwo cieplne ciała stałego (k_s) oraz efektywne przewodnictwo cieplne (k_{ef}) w odniesieniu do przewodnictwa cieplnego płynu (k_f) do analizy jakościowej. Dzięki temu podejściu modele zostały zbadane i sklasyfikowane w cztery podstawowe grupy. W drugiej części pracy porównano wybrane modele z danymi eksperymentalnymi. Eksperymenty obejmowały testowanie ośmiu próbek materiałów porowatych w postaci upakowanych prętów stalowych, ułożonych w dwóch konfiguracjach: przesuniętej i równoległej. Testy przeprowadzono w zakresie temperatury od 75° do 400°C, co odpowiadało stosunkom k_s do k_f w przedziale od 1800 do 855. Do porównywania danych pomiarowych z obliczeniami modelu wykorzystano różne rodzaje reprezentacji graficznych. Wyniki wskazują, że najbardziej dokładne porównania można przeprowadzić za pomocą wykresów liniowych, które prezentują bezwzględne wartości współczynnika k_{ef} w odniesieniu do przewodnictwa cieplnego fazy stałej.

Słowa kluczowe: analiza przewodnictwa cieplnego, materiały porowate, materiały komórkowe, wymiana ciepła